Smart Antenna System Implementation based on Digital Beam-Forming and Software Radio Technologies

J. Wu, W.-X. Sheng, K.-P. Chan, W.-K. Chung, K.-K. M. Cheng, and K.-L. Wu

Department of Electronic Engineering,
The Chinese University of Hong Kong, Shatin, Hong Kong
Phone: (852)2609 8269 Fax: (852)2603 5558 Email: kkcheng@ee.cuhk.edu.hk

Abstract — **This paper presents the design and implementation of a complete receiving smart antenna system. By using software radio techniques, the system can be re-programmed to meet different modulation standards. The platform consists of antenna array, RF module, digital IF module and digital signal processing module. Digital beam-forming and demodulation algorithms are all implemented on DSP. Experimental results are shown for both anechoic chamber and outdoor measurements.**

I. Introduction

The increasing requirement for wireless communication system capacity and limited spectrum resource become rigorous contradictious. A smart antenna is expected to significantly increase the system capacity and the quality of service for wireless communication system [1]. Particularly, a digital beam-forming (DBF) smart antenna offers flexibility because various algorithms can be implemented in DSP. Software radio is another promising technique that enables the digitization of IF signal by high-speed A/D converter and all subsequent processing to be implemented in software. In recent years, much effort has been devoted to the development of smart antenna systems [2-5]. An experimental system has been reported based on analog circuits [2,3]. In [4,5], digital techniques are applied to smart antenna system but the hardware is not capable of real-time processing.

The system to be described here makes use of digital beam-forming and software radio techniques for real-time processing. It is a complete receiving base-station that consists of antenna array, RF module, digital IF module and DSP module. The software part consists of digital beam-forming algorithms and demodulation code for both GMSK and QPSK signals. In this paper, the design, implementation and experimental characterization of the smart antenna system are described.

II. System Overview

Fig. 1 and Table I show, respectively, the block diagram and main specification of the smart antenna system under development.

Table I. Smart Antenna System Specifications

Operating frequency	1920-1980 MHz
Bandwidth	5 MHz
Rx sensitivity	-100 dBm
Dynamic range	80 dB
IF frequency	30 MHz
Sampling rate	40 MHz
Data modulation	GMSK or QPSK
Antenna array	8-element circular array

The antenna array consists of 8 directional antennas that are circularly spaced at equal distance (half-wavelength). In order to be compatible with W-CDMA uplink specification in radio part, the operating frequency and bandwidth are chosen to be 1.92-1.98 GHz and 5MHz, respectively. The RF module function is to down-convert the signal from 1.92-1.98 GHz (RF) to 30MHz (IF). Moreover, RF switches are inserted at the front end for array calibration.

For the software radio part, the 30 MHz IF signal is first digitized by using a high-speed A/D converter, followed by digital down-conversion (DDC). Two stages of cascaded integrator comb (CIC) FIR filters are used for image channel rejection. Data are then transferred from the FIFO to the DSP module for further DBF processing and signal demodulation. Finally, the calculated weighting coefficients of DBF algorithm are passed to a PC through the serial port provided.

III. Hardware Implementation

The photographs of the assembled smart antenna system are given in Fig. 2 & 3. It mainly consists of two racks: one is for the antenna array and RF module; and the other is for the digital IF and DSP circuitry.

A. Antenna array and RF module

Each array element is a printed dipole antenna, as illustrated in Fig. 3(a). This directional antenna has a 3dB

0-7803-7239-5/02/$10.00 © 2002 IEEE

beam width of about 100°. The RF module (Fig. 4) is basically a double-conversion receiver with the RF LO varies from 1.54 to 1.6 GHz and the IF LO equals to 410MHz. The first IF and second IF are 380 MHz and 30 MHz, respectively. An internal calibration source and RF switches are also included here for array calibration. Upon power on, the RF front-end is automatically connected to the reference source for calibration. Once it is completed, the receiver is switched back to the antenna elements for normal operation.

B. Digital IF module

This module includes a high-speed A-to-D Converter, a Digital Down-Converter, a Numerically Controlled Oscillator (NCO), two CIC filters and one Low-Pass Filter (LPF). Parameters such as NCO frequency, CIC filter decimation factor and LPF coefficients are all programmable. The LPF filter can be used as pulse shaping filter. The output data are buffered by using FIFO chips.

C. DSP module

The main task is to perform DBF and demodulation processing on the data received from the FIFO outputs. This module mainly consists of 4 DSP chips (TMS320c6701) and SDRAM. Communication between DSP devices is accomplished by using the Multi-channel Buffered Serial Port (McBSP). All the inter-communication and data exchange are controlled by Direct Memory Access (DMA) to keep the DSP chips running at full speed.

IV. ALGORITHM IMPLEMENTATION

Array calibration, DBF and demodulation algorithms are all performed by DSP devices. This allows the system to be re-programmed for different applications.

A. Array calibration

Most beam-forming algorithms are dependent on the consistency of hardware characteristics. In practice, the phase and gain of the RF elements vary as a function of temperature and time, automatic calibration procedure is therefore required to keep track of parameter variations and to correct them accordingly. If all the reference signals are assumed identical, the calibration coefficients can be estimated by

$$cab\_w_i = y_i / y_1 \qquad i=1, 2,...N \qquad (1)$$

where y_i is the received complex baseband signal. In practice, the amplitude and the phase matching of the calibration signals is dependent on the design of the distribution network. From the measurement, a small amount of parameter mismatch is found to be acceptable by the system.

B. DBF algorithm with phase compensation

Consider an antenna array with N elements. Suppose that the complex envelop of the received RF signal at the antenna element is given as,

$$x_i = s(t)e^{-j\varphi_{si}} \qquad i = 1, 2,...N \qquad (2)$$

where φ_{si} is the phase difference due to array element position. After down-conversion, the received baseband signal from individual channel output is simply

$$y_i = a_i e^{-j\varphi_{ai}} \cdot x_i = s(t) \cdot a_i e^{-j\varphi_i} \qquad (3)$$

where a_i and φ_{ai} is the amplitude and phase associated with the i-th receiving channel; $\varphi_i = \varphi_{si} + \varphi_{ai}$. To maximize the output signal, the weightings of each array antenna element should be chosen as,

$$w_i = e^{j(\varphi_i - \varphi_1)} \qquad i = 1, 2,...N \qquad (4)$$

As a result, the output signal is the constructive sum of the baseband signals from all receiving channels:

$$DBF \quad output = \sum_{i=1}^{N} w_i y_i = s(t)e^{-j\varphi_1} \sum_{i=1}^{N} a_i \qquad (5)$$

The combined radiation pattern of the array antenna may therefore be evaluated by,

$$E(\varphi) = W \cdot Q(\varphi) \qquad (6)$$

where $W = [w_1, w_2, \ldots, w_N]$, $Q(\varphi)$ is the array factor for the array antenna. Expressions of $Q(\varphi)$ for isotropic and non-isotropic antenna element are given by equation (7) and (8),

$$Q(\varphi) = \left[e^{-jkR\cos\varphi}, e^{-jkR\cos(\varphi - \frac{2\pi}{N})}, \cdots, e^{-jkR\cos(\varphi - \frac{(N-1)2\pi}{N})} \right]^T \qquad (7)$$

$$Q(\varphi) = \left[g_1(\varphi)e^{-jkR\cos\varphi}, g_2(\varphi)e^{-jkR\cos(\varphi - \frac{2\pi}{N})}, \cdots, g_N(\varphi)e^{-jkR\cos(\varphi - \frac{(N-1)2\pi}{N})} \right]^T \qquad (8)$$

where $g_i(\varphi)$ is the radiation pattern of the i-th antenna element obtained by numerical analysis or measurements. Fig. 5 shows the radiation pattern for N=8 and Direction of Arrival (DOA) = 0°. The 3dB beam width is about 30° and the side-lobe level is less than –10 dB.

C. Demodulation for GMSK and QPSK

Digital demodulation is carried out that includes I/Q demodulation, carrier and symbol timing synchronization (no analog PLL is used). Both non-coherent GMSK and coherent QPSK demodulators have been implemented.

The GMSK modulated signal can be expressed as,

$$x(t) = A_o \cos[\omega_c t + \phi(t)] \tag{9}$$

where A_o, ω_c and $\phi(t)$ are the carrier amplitude, carrier frequency and the information bearing signal, respectively. In one-bit differential detection, the phase difference is calculated by,

$$\Delta\phi_b(t) = \phi(t) - \phi(t - T_b) \tag{10}$$

Furthermore, the modulation index is set equal to 0.5 and hence the maximum phase change is limited to less than $\pi/2$ within any two bits. This feature can be utilized to construct a digital PLL to compensate for the frequency offset between the transmitter and receiver, whereas the direction of phase change is used to determine the signal levels.

The QPSK modulated signal may be represented by

$$s(t) = \sqrt{2P}\cos[2\pi f_c t + \phi(t) + \theta(t)] + n(t) \tag{11}$$

where P, f_c, $n(t)$ and $\theta(t)$ are the received signal power, carrier frequency, white Gaussian noise and the time-varying phase of the carrier, respectively; $\phi(t)$ is the information bearing signal. For coherent detection, both the carrier frequency offset and phase offset need to be minimized by using either the digital Costas loop or fourth-power loop for carrier phase recovery and automatic frequency correction.

V. Experimental Results

A GMSK modulation signal, with data-rate of 26.667 kbit/s and carrier frequency of 1.95GHz, is used in the study. At the receiver side, the data-rate is 266.67 kbit/s after DDC and 3 stages of decimated LPF (over-sampling rate = 10). The antenna array weightings are updated every 50 samples (about 187μs).

The first experiment is conducted in a RF anechoic chamber, and the array antenna patterns thus obtained are plotted in Fig. 6. It is observed that a beam are formed pointing toward the DOA of the transmitter and can track it adaptively. The beam width is also in good agreement with the predicted value. The second experiment is carried out in an open space environment and the measurement results are given in Fig. 7. The main beam is also directed towards the transmitter, but a side lobe is also found due to the reflections from nearby buildings. Multi-path effect may be overcome by using equalizer or rake receiver.

VI. Conclusion

The implementation and performance of a complete smart antenna system based on real-time digital signal processing approach is described. Due to the speed limitation of the DSP I/O, this platform is unable to support CDMA signal due to the high chip rate required. An enhanced model is under development that will include uplink and downlink capability as well as FPGA implementation for wideband CDMA application.

Acknowledgement

The authors would like to thank the Innovation and Technology Commission (ITC) of Hong Kong SAR for their financial support.

References

[1] Joseph C. Liberti, J., and Theodore S. R., "Smart Antennas for Wireless Communications", Upper Saddle River: Prentice Hall PTR, 1999.

[2] Okamoto G., "Smart Antenna System and Wireless LANs", Kluwer Academic Publishers, 1999.

[3] Jeng S., Okamoto G., and Xu G., "Experimental evaluation of smart antenna system performance for capacity improvement," 1997 IEEE GLOBECOM, vol. 1, pp. 369-373.

[4] Matsuoka. H., Murakami Y., Shoki H., and Suzuki Y., "A smart antenna receiver testbed with directional antenna elements," 2000 IEEE Int. Conference on Phased Array Systems and Technology, pp.: 113-116.

[5] Im H., and Choi S., "Implementation of a smart antenna test-bed," 2000 IEEE Antennas and Propagation Society Int. Symp., vol. 2 , pp.: 952-955.

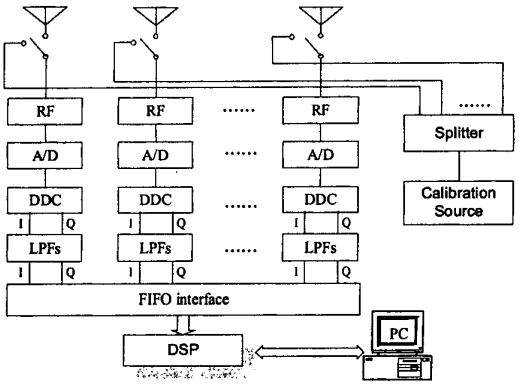

Fig.1. Block Diagram of smart antenna testbed

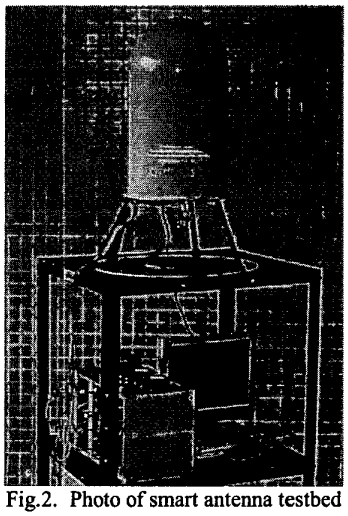

Fig.2. Photo of smart antenna testbed

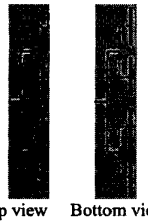

Top view Bottom view

Fig.3a. Antenna element

3b. RF Module

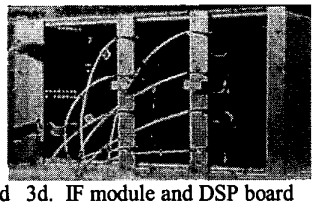

Fig.3c. Individual RF board 3d. IF module and DSP board

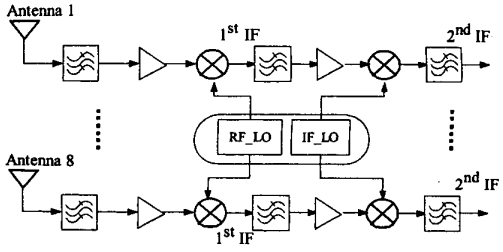

Fig.4. Block diagram of RF module

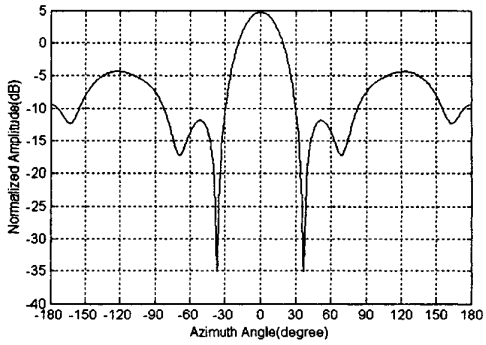

Fig.5. Array antenna pattern of circular array with 8 directional elements, DOA is 0°.

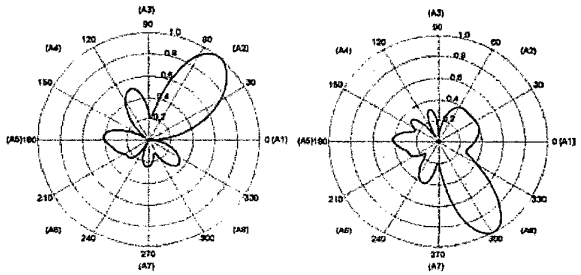

DOA=50° DOA=296°

Fig.6. Array antenna pattern in anechoic chamber

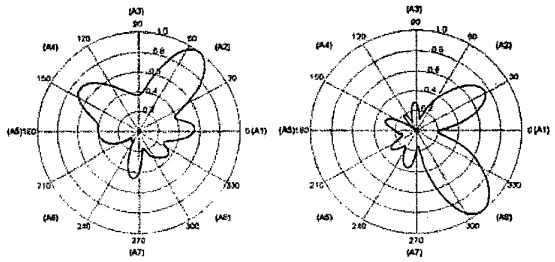

DOA=48° DOA=293°

Fig.7. Array antenna pattern outdoor